2023 62nd IEEE Conference on Decision and Control (CDC)
December 13-15, 2023. Marina Bay Sands, Singapore

LMI-based Stability Analysis of a Geometric PID-type Attitude Control Law

Farooq Aslam, Hafiz Zeeshan Iqbal Khan, M. Farooq Haydar, Suhail Akhtar, and Jamshed Riaz

***Abstract*— This paper presents an analytical framework for analyzing the stability of a geometric PID controller, with a prescribed structure, for attitude control on the Special Orthogonal Group $SO(3)$. A key feature of the proposed approach is the use of linear matrix inequalities (LMIs) to formulate sufficient conditions which ensure that the closed-loop tracking error system is almost globally asymptotically stable (AGAS). To this end, a candidate Lyapunov function is considered which is slightly more general than those traditionally employed in the $SO(3)$ literature. In particular, the Lyapunov function contains terms which couple the attitude and velocity errors with the integrator state, as well as matrix gains for four of the six Lyapunov function coefficients. The LMI-based stabilization conditions are then cast as a feasibility problem which can be used to search for Lyapunov function coefficients that confirm AGAS for a given PID controller with matrix gains. Using the proposed approach, control designers can use linearized models of the attitude kinematics and dynamics to tune the PID gains, and then solve a semidefinite programming problem to obtain AGAS guarantees for the corresponding geometric nonlinear PID controller. The effectiveness of this method is demonstrated on a practical problem involving the design and analysis of a geometric PID controller for a hexacopter UAV with local performance requirements specified in terms of rise time, settling time, gain and phase margins, and closed-loop bandwidth.**

***Index Terms*— Attitude control, geometric PID control, almost global asymptotic stability (AGAS), Special Orthogonal Group $SO(3)$, linear matrix inequalities**

I. Introduction

The attitude of an object rotating in three-dimensional space is described globally and uniquely by the rotation matrix parameterization [1]. Rotation matrices are elements of a matrix Lie group known as the Special Orthogonal Group $SO(3)$. This is the set of real, orthogonal, 3-by-3 matrices with determinant 1. Due to the complex nonlinear geometry of rotational motion, geometric nonlinear control methods which work directly with rotation matrices are becoming increasingly popular [2]. In particular, the globally defined and unique nature of the rotation matrix parameterization ensures that geometric nonlinear controllers do not suffer from singularities or unwinding, limitations that often arise with other commonly-used attitude parameterizations such as Euler angles, Rodrigues parameters, and quaternions [1].

Several researchers have addressed the problem of attitude and position control on the matrix Lie groups $SO(3)$ and $SE(3)$. The latter denotes the Special Euclidean Group, and encodes both the rotational and translational positions for an object moving in three-dimensional space. Geometric PD and PID controllers have received significant attention (see [3], [4], [5], [6], [7], [8] and the references therein). These controllers typically use fixed gains for the attitude and velocity error correction terms, and integral action to compensate for constant, or slowly-varying, disturbances. Almost global asymptotic stability (AGAS) guarantees are usually obtained using Lyapunov stability theory. However, the Lyapunov analysis is often simplified either by using scalar gains in the PID controller and/or scalar coefficients in the Lyapunov function, or by fixing certain Lyapunov function coefficients. The latter situation arises when some of the Lyapunov coefficients are specified in terms of the gains used in the PID controller, or when certain cross-terms are omitted (by setting the corresponding coefficients to zero).

Similarly, the choice of input signal to the integrator can also help simplify the Lyapunov analysis. A case in point is the geometric PID controller proposed in [6]. There, the integrator state is eliminated from the Lyapunov rate by choosing the integrator input as a particular linear combination of the attitude and velocity errors. Although the elimination of the integrator state from the Lyapunov rate helps simplify the Lyapunov analysis, it does so by imposing the requirement that both the attitude *and* velocity errors be input to the integrator. Thus, the PID controller in [6] excludes control architectures which do not use velocity feedback in the integrator input. Examples of such controllers include cascade PI/P controllers often employed in flight control systems such as pitch-attitude hold autopilots ([9], Section 4.6). In these control systems, an outer loop PI compensator (or a lag filter) tracks attitude commands, whereas a proportional gain in the inner (rate) loop provides the necessary damping.

Another potential limitation of existing geometric PID controllers arises in the context of digital control systems and pure integrators. More precisely, when pure integrators are discretized, the corresponding discrete-time pole lies exactly on the boundary of the unit disc, i.e., at the $(1, 0)$ point. The resulting discrete-time controller is only marginally stable, and may produce undesirable effects due to, for instance, limited numerical precision. In practice, a way around this problem is to shift the pole of the continuous-time integrator slightly to the left of the origin so that the corresponding discrete-time pole lies strictly inside the unit disc. For a geometric PID controller, this means that the input to the integrator includes negative feedback of the integrator state using a small gain.

Motivated by the various practical concerns outlined

Farooq Aslam, Hafiz Zeeshan Iqbal Khan, Muhammad Farooq Haydar, Suhail Akhtar, and Jamshed Riaz are with the Institute of Space Technology, Islamabad, Pakistan. Hafiz Zeeshan Iqbal Khan is also with the Centers of Excellence in Science and Applied Technologies, Islamabad, Pakistan (Corresponding author: farooq.aslam87@gmail.com)

above, our goal in this paper is to analyze the closed-loop stability of a geometric PID controller which uses matrix gains and a prescribed architecture for the integrator. More precisely, the input signal to the integrator includes negative feedback of the integrator state and excludes velocity feedback. As this paper demonstrates, closed-loop stability guarantees for the resulting geometric PID controller can be obtained by extending existing analytical frameworks, and by considering a slightly more general Lyapunov function than is traditionally considered in the $SO(3)$ literature. In particular, we consider a candidate Lyapunov function which includes cross-terms coupling the attitude *and* velocity errors with the integrator state. Thereafter, we express the stabilization conditions in the form of matrix inequalities in which the various submatrices are linear functions of the unknown Lyapunov function coefficients. The resulting linear matrix inequalities (LMIs) are then used to formulate a feasibility problem with the aim of finding Lyapunov function coefficients which ensure that the closed-loop system is almost globally asymptotically stable (AGAS). Using the proposed approach, control designers can use linearized models of the attitude kinematics and dynamics to tune the PID gains, and then solve a semidefinite programming problem to obtain AGAS guarantees for the corresponding geometric nonlinear PID controller. Lastly, we demonstrate the applicability of our approach on a practical problem involving the design and analysis of a geometric PID controller for a hexacopter UAV with local performance requirements specified in terms of rise time, settling time, gain and phase margins, and closed-loop bandwidth.

The rest of the paper is structured as follows: after Section II describes the notation and basic concepts used in the paper, Section III introduces the attitude control problem and the geometric PID controller under consideration. A detailed stability analysis of the closed-loop tracking error system is carried out in Section IV, and the main results of the paper are presented. Section V describes the case study, before Section VI concludes the discussion.

II. Preliminaries

For vectors $x, y \in \mathbb{R}^n$, let $x \cdot y = x^\top y$ denote the standard inner (or dot) product, and let $||x|| = \sqrt{x \cdot x}$ denote the Euclidean norm. For a matrix $M \in \mathbb{R}^{n\times m}$, the induced 2-norm $||M||$ is given by $||M|| = \sqrt{\lambda_{\max}(M^\top M)}$, where $\lambda_{\max}(\cdot)$ represents the largest eigenvalue of a matrix. The Special Orthogonal group $SO(3)$ is the set of real, 3×3, orthogonal matrices with determinant 1, that is,

$$SO(3) = \left\{R \in \mathbb{R}^{3\times 3} : R^\top R = I, \det(R) = 1\right\}.$$

For vectors $x, y \in \mathbb{R}^3$, the *cross* product satisfies $x \times y = x^\times y$, where

$$x^\times = \begin{bmatrix} x_1 \\ x_2 \\ x_3 \end{bmatrix}^\times := \begin{bmatrix} 0 & -x_3 & x_2 \\ x_3 & 0 & -x_1 \\ -x_2 & x_1 & 0 \end{bmatrix}.$$

The inverse of the cross ($\times$) operator, denoted by the *vee* ($\vee$) operator, extracts the entries of the vector x from the skew-symmetric matrix $x^\times$, i.e., $(x^\times)^\vee = x$. Lastly, the cross and vee operators satisfy the following identities [5]:

$$x^\times y = x \times y = -y \times x = -y^\times x, \tag{1a}$$
$$\text{tr}[Ax^\times] = -x \cdot (A - A^\top)^\vee, \tag{1b}$$
$$x^\times A + A^\top x^\times = \left(\{\text{tr}[A]I - A\}\, x\right)^\times, \tag{1c}$$
$$Rx^\times R^\top = (Rx)^\times, \tag{1d}$$

for any $x, y \in \mathbb{R}^3$, $A \in \mathbb{R}^{3\times 3}$, and $R \in SO(3)$.

III. Problem Formulation

This section formulates the attitude control problem under consideration. Rigid-body rotational motion is modeled as:

$$\begin{aligned} \dot{R} &= R\omega^\times, \\ J\dot{\omega} &= -\omega^\times J\omega + \tau, \end{aligned} \tag{2}$$

where $R \in SO(3)$ describes the orientation of the body-fixed frame relative to the inertial frame, $\omega \in \mathbb{R}^3$ is the angular velocity expressed in body coordinates, $J = J^\top > 0$ is the inertia matrix, and $\tau \in \mathbb{R}^3$ is the applied torque. In order to formulate the reference tracking problem, we consider a reference attitude which obeys the kinematics:

$$\dot{R}_d = R_d\omega_d^\times, \tag{3}$$

where $\omega_d \in \mathbb{R}^3$ is the desired angular velocity which is bounded and whose time derivative, $\dot{\omega}_d$, is also bounded. The attitude and velocity errors are defined as follows:

$$R_e := R_d^\top R, \qquad \omega_e := \omega - R_e^\top \omega_d. \tag{4}$$

In addition, we define the attitude error vector as:

$$e_R := \frac{1}{2}(R_e - R_e^\top)^\vee. \tag{5}$$

From (2)-(4), we obtain the tracking error system:

$$\begin{aligned} \dot{R}_e &= R_e\omega_e^\times \\ J\dot{\omega}_e &= -\omega^\times J\omega + \tau + J\omega_e^\times R_e^\top \omega_d - JR_e^\top \dot{\omega}_d \end{aligned} \tag{6}$$

Next, we consider the following control torque:

$$\tau = u + u_C, \tag{7}$$

where $u \in \mathbb{R}^3$ is the feedback component of the applied torque, and $u_C \in \mathbb{R}^3$ is a cancellation torque which compensates for the gyroscopic coupling $\omega^\times J\omega$ as well as the contribution of the terms containing $(\omega_d, \dot{\omega}_d)$. More precisely, the cancellation torque is given as

$$u_C := \omega^\times J\omega - J\omega_e^\times R_e^\top \omega_d + JR_e^\top \dot{\omega}_d. \tag{8}$$

Lastly, we consider the following PID-type feedback:

$$\begin{aligned} u &= -K_P e_R - K_D\omega_e - K_I e_I, \\ \dot{e}_I &= -T_I e_I + e_R, \end{aligned} \tag{9}$$

where the matrices $(K_P, K_D, K_I, T_I) \in \mathbb{R}^{3\times 3}$ are symmetric positive definite and assumed to be known. Consequently,

the closed-loop tracking error system with the control torque (7)-(9) is obtained as:

$$\begin{aligned} \dot{R}_e &= R_e \omega_e^{\times} \\ J\dot{\omega}_e &= -K_P e_R - K_D \omega_e - K_I e_I \\ \dot{e}_I &= -T_I e_I + e_R \end{aligned} \tag{10}$$

In the next section, we will analyze the closed-loop stability of the tracking error system (10). In particular, we will derive sufficient conditions in the form of linear matrix inequalities which can be used to check whether the PID controller (9) almost globally asymptotically stabilizes the desired equilibrium $(R_e, \omega_e, e_I) = (I, 0, 0)$.

Remark 1: The PID controller (9) includes cascade controllers in which an outer attitude loop uses PI-type compensation to track attitude commands and an inner velocity loop uses proportional feedback to generate the necessary damping. More precisely, consider the control law

$$u = K_\omega(\omega_{\text{ref}} - \omega), \tag{11}$$

where $\omega_{\text{ref}} = u_R + R_e^\top \omega_d$ is the velocity reference generated by the attitude loop, and u_R is the output of the following PI-type compensator:

$$u_R = -K_R e_R - K_I e_I, \quad \dot{e}_I = -T_I e_I + e_R. \tag{12}$$

We observe that:

$$u = K_\omega(u_R + R_e^\top \omega_d - \omega) = K_\omega(u_R - \omega_e).$$

The cascade controller can then be expressed as:

$$\begin{aligned} u &= -K_\omega K_R e_R - K_\omega \omega_e - K_\omega K_I e_I, \\ \dot{e}_I &= -T_I e_I + e_R. \end{aligned} \tag{13}$$

Thus, the results presented in this paper also hold for the cascade controller (11)-(12).

IV. Main Results

A. Attitude error function

In order to analyze the closed-loop stability of the tracking error system (10), we consider the following attitude error function:

$$\Psi = \frac{1}{2}\text{tr}[I - R_e] \tag{14}$$

Its time derivative is obtained as:

$$\dot{\Psi} = -\frac{1}{2}\text{tr}[\dot{R}_e] = -\frac{1}{2}\text{tr}[R_e \omega_e^{\times}] = \frac{1}{2}\omega_e \cdot (R_e - R_e^\top)^{\vee},$$

where we have used the identity (1b). Using the expression for the attitude error vector (5), we observe that:

$$\dot{\Psi} = e_R \cdot \omega_e \tag{15}$$

Next, we obtain the time derivative of the attitude error vector:

$$\begin{aligned} \dot{e}_R^{\times} &= \frac{1}{2}(\dot{R}_e - \dot{R}_e^\top) = \frac{1}{2}(R_e \omega_e^{\times} + \omega_e^{\times} R_e^\top) \\ &= \frac{1}{2}\{(\text{tr}[R_e] I - R_e^\top)\omega_e\}^{\times}, \end{aligned}$$

where the last equality follows from the identity (1c). Consequently, we express the rate of change of the attitude error vector as:

$$\dot{e}_R = E(R_e)\omega_e, \tag{16}$$

where the mapping $E : \mathbb{R}^{3\times 3} \to \mathbb{R}^{3\times 3}$ is defined as follows:

$$E(M) := \frac{1}{2}(\text{tr}[M] I - M^\top) \tag{17}$$

We recall that the attitude error $R_e \in SO(3)$ can be expressed as:

$$R_e = I + (\sin\theta_e)\alpha^{\times} + (1 - \cos\theta_e)\alpha^{\times}\alpha^{\times},$$

where $(\theta_e, \alpha) \in \mathbb{R} \times S^2$ represent the angle of rotation and the axis of rotation, respectively. Moreover, using the MATLAB Symbolic Computation Tool, we observe that the eigenvalues of the matrix $E^\top(R_e)E(R_e)$ are given by:

$$\frac{1}{2}(1 + \cos\theta_e), \quad \frac{1}{2}(1 + \cos\theta_e), \quad \cos^2\theta_e.$$

Therefore, the matrix 2-norm satisfies $||E(R_e)|| \leq 1$.

B. Lyapunov function

Next, we use the attitude error function (14) to define the following candidate Lyapunov function:

$$\begin{aligned} V := {} & 2p_{11}\Psi + \omega_e \cdot P_{22} J\omega_e + 2p_{21} e_R \cdot J\omega_e \\ & + e_I \cdot P_{33} e_I + 2e_I \cdot P_{31} e_R + 2e_I \cdot P_{32} J\omega_e \end{aligned} \tag{18}$$

In the above expression, $p_{11} > 0$ and $p_{21} \geq 0$ represent scalars, and $(P_{31}, P_{32}, P_{22}, P_{33}) \in \mathbb{R}^{3\times 3}$ denote matrices, with $P_{22}J$ and P_{33} being symmetric positive definite. We note that the matrices (P_{31}, P_{32}) couple the integrator state e_I with the attitude and velocity errors (e_R, ω_e). Moreover, using the fact that ([6], Proposition 1)

$$\Psi \geq \frac{1}{2}||e_R||^2,$$

we bound the Lyapunov function as:

$$V \geq x^\top \mathcal{P} x, \tag{19}$$

where

$$x := \begin{bmatrix} e_R \\ \omega_e \\ e_I \end{bmatrix}, \qquad \mathcal{P} := \begin{bmatrix} p_{11} I & * & * \\ p_{21} J & P_{22} J & * \\ P_{31} & P_{32} J & P_{33} \end{bmatrix}. \tag{20}$$

Consequently, a sufficient condition for V to be positive definite is given as:

$$\mathcal{P} > 0, \qquad p_{21} \geq 0. \tag{21}$$

Remark 2: Before proceeding further with the analysis, we compare the candidate Lyapunov function (18) with that used in [6]. In particular, the Lyapunov function considered in [6] can be expressed as:

$$V_L = k_P \Psi + \frac{1}{2}\omega_e \cdot J\omega_e + c_2 e_R \cdot J\omega_e + \frac{1}{2}k_I e_I \cdot e_I, \tag{22}$$

where (k_P, k_I) are positive scalars employed in the proportional and integral terms of the geometric nonlinear PID-type attitude control law proposed in [6]. Comparing (18)

and (22), we observe that the latter is a special case of the former. In particular, by setting $p_{11} = k_P/2$, $P_{22} = (1/2)I$, $p_{21} = c_2/2$, $P_{33} = (k_I/2)I$, and $P_{31} = P_{32} = 0$, we obtain the Lyapunov function (22). Moreover, for the closed-loop tracking error system considered in [6], the Lyapunov rate $\dot{V}_L$ contains three terms involving the integrator state e_I. These terms are given by

$$\dot{e}_I \cdot (k_I e_I) + (\omega_e + c_2 e_R) \cdot (-k_I e_I),$$

and their contribution to the Lyapunov rate is easily cancelled if the integrator input is set as

$$\dot{e}_I = \omega_e + c_2 e_R. \tag{23}$$

This is precisely the choice made in [6] and requires that both tracking errors (e_R, ω_e) be input to the integrator (23). As a result, this approach precludes the use of control architectures, such as cascade PI/P controllers, in which integral action or lag compensation is performed in the outer attitude loop, and only proportional feedback is used in the inner velocity loop. For such control architectures, it may be advantageous to use a more general Lyapunov function such as the one considered in (18).

Proposition 1: Consider the closed-loop tracking error system (10) and the candidate Lyapunov function (18). Let λ_J denote the largest eigenvalue of the inertia matrix J. Then, the Lyapunov rate along trajectories of (10) satisfies the following relation:

$$\dot{V} \leq x^\top (\mathcal{M} + \mathcal{Q}) x, \tag{24}$$

where

$$\mathcal{M} := \begin{bmatrix} M_{11} & * & * \\ M_{21} & M_{22} & * \\ M_{31} & M_{32} & M_{33} \end{bmatrix}, \quad \mathcal{Q} := \begin{bmatrix} 0 & * & * \\ 0 & 0 & * \\ 0 & P_{31}E(R_e) & 0 \end{bmatrix}, \tag{25}$$

and the submatrices M_{ij} are defined as follows:

$$M_{11} := -2p_{21}K_P + (P_{31} + P_{31}^\top), \tag{26a}$$
$$M_{22} := -2P_{22}K_D + 2p_{21}\lambda_J I, \tag{26b}$$
$$M_{33} := -2P_{33}T_I - (P_{32}K_I + K_I P_{32}^\top), \tag{26c}$$
$$M_{21} := p_{11}I - p_{21}K_D - P_{22}K_P + JP_{32}^\top, \tag{26d}$$
$$M_{31} := P_{33} - p_{21}K_I - T_I P_{31} - P_{32}K_P, \tag{26e}$$
$$M_{32} := -P_{32}K_D - K_I P_{22} - T_I P_{32} J. \tag{26f}$$

Proof: See Appendix. ∎

Proposition 1 gives an upper bound (24) for the Lyapunov rate $\dot{V}$. Using this bound, we obtain the following sufficient condition for $\dot{V}$ to be negative definite:

$$\mathcal{M} + \mathcal{A} < 0, \tag{27a}$$
$$\mathcal{Q} - \mathcal{A} < 0, \tag{27b}$$

where $\mathcal{A} \in \mathbb{R}^{9\times 9}$ is a block diagonal matrix, with symmetric positive definite blocks, defined as follows:

$$\mathcal{A} := \begin{bmatrix} A_1 & 0 & 0 \\ 0 & \alpha_2 I & 0 \\ 0 & 0 & A_3 \end{bmatrix}, \qquad A_1, A_3 \in \mathbb{R}^{3\times 3}, \tag{28}$$

and α_2 is a positive scalar. Substituting the expression for $\mathcal{Q}$, given in (25), we restate (27b) as:

$$-A_1 < 0, \qquad \begin{bmatrix} -\alpha_2 I & E^\top(R_e)P_{31}^\top \\ P_{31}E(R_e) & -A_3 \end{bmatrix} < 0. \tag{29}$$

Then, taking the Schur complement, we restate (29) as:

$$A_1, A_3 > 0, \qquad \alpha_2 I - E^\top P_{31}^\top A_3^{-1} P_{31} E > 0. \tag{30}$$

Next, we recall that the largest singular value of the matrix $E(R_e)$ is 1. Moreover, since α_2 is positive, we obtain the following sufficient condition for (30):

$$A_1, A_3 > 0, \qquad E^\top(\alpha_2 I - P_{31}^\top A_3^{-1} P_{31})E > 0. \tag{31}$$

Lastly, applying the Schur complement lemma, we obtain the following sufficient condition for (31):

$$A_1 > 0, \qquad \begin{bmatrix} \alpha_2 I & * \\ P_{31} & A_3 \end{bmatrix} > 0. \tag{32}$$

This brings us to the main result of the paper.

Theorem 1: Consider the closed-loop tracking error system (10), the candidate Lyapunov function (18), and the matrices $(\mathcal{P}, \mathcal{M}, \mathcal{A})$, defined in (20), (25)-(26) and (28), respectively. Suppose that there exist Lyapunov function coefficients (p_{11}, p_{21}, P_{ij}) such that the LMIs (21), (27a), and (32) are satisfied. Then, the desired equilibrium $(R_e, \omega_e, e_I) = (I, 0, 0)$ of the closed-loop tracking error system (10) is almost globally asymptotically stable.

Proof: The condition (21) ensures that the candidate Lyapunov function (18) is positive definite. The condition (32) ensures that (27b) holds, which, together with (27a) ensures that the Lyapunov rate $\dot{V}$ is negative definite. As a result, the tracking errors (e_R, ω_e, e_I) converge asymptotically to zero. Moreover, it can be shown, using similar arguments as in ([10], Appendix A), that the undesired equilibria are unstable, and that almost all the trajectories of the closed-loop tracking error system (10) converge to the desired equilibrium $(R_e, \omega_e, e_I) = (I, 0, 0)$. ∎

Remark 3: Theorem 1 formulates a feasibility problem which can be used to analyze the closed-loop stability of a given geometric nonlinear PID controller of the form (9). Moreover, the LMI-based formulation can be used in conjunction with linearization-based methods for tuning the controller gains. More precisely, in the first step, a control designer can use linearized models for the attitude kinematics and dynamics to tune the matrix gains (K_P, K_D, K_I, T_I) such that the linearized closed-loop error system satisfies local stability and performance criteria. Then, in the second step, the designer can solve the feasibility problem in Theorem 1 to search for Lyapunov function coefficients which guarantee almost global asymptotic stability for the closed-loop tracking error system (10). This two-step approach is detailed using the case study in Section V.

Remark 4: The Lyapunov function (18) employs the same Morse-Bott function as used in the stability analysis carried out in [6], and the gradient of this function is used by the controller (9). As a result, all orientations with an angle of rotation equal to $\pm\pi$ radians are equilibria of the

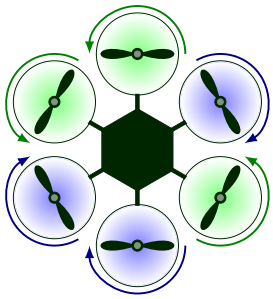

Fig. 1. A hexacopter configuration

resulting closed-loop tracking error system (10). The domain of attraction can be improved by replacing the Morse-Bott function by a Morse function such as the one used in [8]. In this case, the domain of attraction will encompass all orientations except for those corresponding to three isolated undesired equilibria.

V. Case Study

In this section, we consider the problem of designing a geometric PID-type attitude controller for a multicopter. In particular, we use decoupled single-axis linearized models to tune the controller gains. Then, we verify that the controller gains satisfy the stabilization conditions given in Theorem 1, and apply these gains in the geometric controller (9).

A. Controller Design

For our case study, we consider the hexacopter depicted in Fig. 1. Its inertia matrix is as follows:

$$J = \begin{bmatrix} 0.0411 & 0 & 0 \\ 0 & 0.0478 & 0 \\ 0 & 0 & 0.0599 \end{bmatrix} \text{ kg/m}^2.$$

Furthermore, for the purposes of controller design, we consider the following decoupled single-axis linearized models for the three axes:

$$\begin{aligned} \dot{\xi}_i &= \omega_i \\ J_i \dot{\omega}_i &= -k_{P_i} \xi_i - k_{D_i} \omega_i - k_{I_i} e_{I,i} \\ \dot{e}_{I,i} &= -\varepsilon_i e_{I,i} + \xi_i \end{aligned} \tag{33}$$

Here, $J_i > 0$ denotes the principal inertia about the i-th body-frame axis, ω_i denotes the angular velocity about the corresponding axis, and $(k_P, k_D, k_I, \varepsilon)_i$ represent positive controller gains.

For each attitude axis, we design controllers which meet the following specifications:

1) Closed-loop bandwidth of approximately 5 rad/s;
2) Rise time < 0.5 s;
3) Settling time (2% criterion) < 5 s;
4) Phase margin $> 60^\circ$ and gain margin > 6 dB.

The controller gains are summarized in Table I. These gains have been selected such that they yield approximately identical closed-loop properties for the roll, pitch, and yaw axes. These properties are listed in Table II, and indicate that the corresponding controllers satisfy the design specifications. We complete the design by confirming that these gains satisfy the stabilizations conditions given in Theorem 1. More precisely, we use the YALMIP and SeDuMi toolboxes to verify that the LMIs (21), (27a), and (32) define a feasible constraint set. Consequently, we conclude that for the hexacopter model under consideration, the geometric nonlinear PID controller (9), implemented using the gains in Table I, almost globally asymptotically stabilizes the closed-loop tracking error system (10).

TABLE I

Controller gains used in (9).

Gain	Values
K_P	$\text{diag}(6.1217; 7.1198; 8.9219)$
K_D	$\text{diag}(1.4284; 1.6613; 2.0818)$
K_I	$\text{diag}(0.7754; 0.9018; 1.1301)$
T	$\text{diag}(0.001; 0.001; 0.001)$

TABLE II

Closed-loop properties for the gains in Table I.

Property	Value
Rise time [s]	0.416
Settling time [s]	3.67
Overshoot [%]	2.57
Gain margin [dB]	48.8
Phase margin [°]	83.02
Loop crossover [rad/s]	35
Closed-loop bandwidth [rad/s]	5.003

B. Regulation & Disturbance Rejection

In this section, we demonstrate the disturbance rejection and attitude regulation capability of the geometric PID controller (9) designed in Section V-A, and compare the performance of this controller with that of the geometric PID controller proposed in [6]. Although the latter controller uses scalar gains as opposed to the matrix gains employed in (9), we select these gains in such a way that the two controllers have similar closed-loop performance. In particular, we tune the latter controller so that the closed-loop bandwidths for the roll, pitch, and yaw channels equal $(5.024, 5.115, 5.281)$ rad/s. This allows us to obtain a fair comparison between the two controllers.

We consider an initial condition for which the pitch error equals 170°, and the roll and yaw errors are zero. In addition, we assume that a constant disturbance torque of $(0, 1, 0)^\top$ Nm perturbs the attitude dynamics in (2). Both controllers are tasked with regulating the attitude to the desired equilibrium $R = I$ and rejecting the constant (but unknown) disturbance. For plotting the results, we resort to the axis-angle representation. In particular, Fig. 2 depicts the angle of rotation attained by both controllers as they regulate the attitude. The plots demonstrate that both the lag compensator-based design (33) and the pure integrator-based design [6] achieve similar performance in terms of attitude regulation and disturbance rejection. Moreover, the pure integrator exhibits a long 'tail' whilst regulating the error to zero, whereas the lag compensator reduces the error

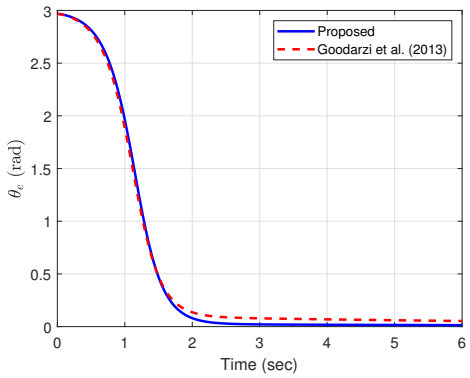

Fig. 2. Angle (axis-angle representation) - Regulation & disturbance rejection

to approximately 0.001 at steady-state, i.e., to a steady-state error of approximately 0.1%.

VI. Conclusion

This paper developed an analytical framework, based on linear matrix inequalities (LMIs) and convex optimization, for analyzing the stability of a PID-type attitude control law, with a prescribed structure, on the matrix Lie group $SO(3)$. We hope that the approach presented herein will provide practitioners with a more general framework for analyzing the stability of geometric PID controllers for attitude control problems. As demonstrated in the case study, control engineers can use this approach to design separate PID controllers for each axis and then solve a feasibility problem, via semidefinite programming, to confirm that the closed-loop system, using a geometric PID controller with the same gains, almost globally asymptotically stabilizes the desired equilibrium. Moreover, we hope that our approach will add to existing results on the use of convex optimization for the analysis and design of geometric nonlinear attitude control laws [11], [12], [13]. In future work, we hope to extend the analytical framework presented here so that it also includes performance considerations and yields a design procedure which can be used to synthesize geometric nonlinear PID controllers for attitude control applications.

Appendix

Proof of Proposition 1

Proof: The time derivative of the candidate Lyapunov function (18) is given by:

$$\begin{aligned}\dot{V} &= 2p_{11}\dot{\Psi} + 2\omega_e \cdot P_{22}J\dot{\omega}_e + 2p_{21}e_R \cdot J\dot{\omega}_e \\ &\quad + 2p_{21}\dot{e}_R \cdot J\omega_e + 2e_I \cdot P_{33}\dot{e}_I + 2e_I \cdot P_{31}\dot{e}_R \\ &\quad + 2\dot{e}_I \cdot P_{31}e_R + 2e_I \cdot P_{32}J\dot{\omega}_e + 2\dot{e}_I \cdot P_{32}J\omega_e \\ &= 2p_{11}\dot{\Psi} + 2(p_{21}e_R + P_{22}\omega_e + P_{32}^\top e_I) \cdot J\dot{\omega}_e \\ &\quad + 2p_{21}\dot{e}_R \cdot J\omega_e + 2e_I \cdot P_{31}\dot{e}_R \\ &\quad + 2(P_{31}e_R + P_{32}J\omega_e + P_{33}e_I) \cdot \dot{e}_I\end{aligned}$$

Substituting the equations for the closed-loop tracking error system (10), we simplify the Lyapunov rate as:

$$\begin{aligned}\dot{V} &= 2p_{11}e_R \cdot \omega_e - 2p_{21}e_R \cdot (K_P e_R + K_D\omega_e + K_I e_I) \\ &\quad - 2(P_{22}\omega_e + P_{32}^\top e_I) \cdot (K_P e_R + K_D\omega_e + K_I e_I) \\ &\quad + 2p_{21}\omega_e \cdot JE(R_e)\omega_e + 2e_I \cdot P_{31}E(R_e)\omega_e \\ &\quad + 2(P_{31}e_R + P_{32}J\omega_e + P_{33}e_I) \cdot (-Te_I + e_R)\end{aligned}$$

Re-arranging terms, we obtain:

$$\begin{aligned}\dot{V} &= -2p_{21}e_R \cdot K_P e_R + 2e_R \cdot P_{31}e_R - 2\omega_e \cdot P_{22}K_D\omega_e \\ &\quad + 2e_R \cdot (p_{11}I - p_{21}K_D - K_P P_{22} + P_{32}J)\omega_e \\ &\quad - 2e_I \cdot P_{33}Te_I - 2e_I \cdot P_{32}K_I e_I \\ &\quad - 2e_I \cdot (p_{21}K_I + TP_{31} + P_{32}K_P - P_{33})e_R \\ &\quad - 2e_I \cdot (P_{32}K_D + K_I P_{22} + TP_{32}J)\omega_e \\ &\quad + 2p_{21}\omega_e \cdot JE(R_e)\omega_e + 2e_I \cdot P_{31}E(R_e)\omega_e\end{aligned}$$

Since $p_{21} \geq 0$ and the largest singular value of $E^\top(R_e)E(R_e)$ is 1, we can bound the second-last term as follows:

$$p_{21}\omega_e \cdot JE(R_e)\omega_e \leq p_{21}\lambda_J||\omega_e||^2,$$

where λ_J denotes the largest eigenvalue of the inertia matrix J. Using this relation, we obtain the bound (24) for the Lyapunov rate. ■

References

[1] N. A. Chaturvedi, A. K. Sanyal, and N. H. McClamroch, "Rigid-body attitude control," *IEEE Control Systems Magazine*, vol. 31, no. 3, pp. 30–51, 2011.

[2] F. Bullo and A. D. Lewis, *Geometric Control of Mechanical Systems: Modeling, Analysis, and Design for Simple Mechanical Control Systems*. Springer, 2019.

[3] F. Bullo and R. M. Murray, "Proportional derivative (PD) control on the Euclidean group," 1995.

[4] T. Lee, M. Leok, and N. H. McClamroch, "Geometric tracking control of a quadrotor UAV on $SE(3)$," in *49th IEEE Conference on Decision and Control (CDC)*. IEEE, 2010, pp. 5420–5425.

[5] T. Lee, "Geometric tracking control of the attitude dynamics of a rigid body on $SO(3)$," in *Proceedings of the 2011 American Control Conference*, 2011, pp. 1200–1205.

[6] F. Goodarzi, D. Lee, and T. Lee, "Geometric nonlinear PID control of a quadrotor UAV on $SE(3)$," in *2013 European Control Conference (ECC)*. IEEE, 2013, pp. 3845–3850.

[7] D. S. Maithripala and J. M. Berg, "An intrinsic PID controller for mechanical systems on Lie groups," *Automatica*, vol. 54, pp. 189–200, 2015.

[8] H. Eslamiat, N. Wang, R. Hamrah, and A. K. Sanyal, "Geometric integral attitude control on $SO(3)$," *Electronics*, vol. 11, no. 18, p. 2821, 2022.

[9] B. L. Stevens, F. L. Lewis, and E. N. Johnson, *Aircraft Control and Simulation: Dynamics, Controls Design, and Autonomous Systems*, 3rd ed. John Wiley & Sons, 2015.

[10] F. Goodarzi, D. Lee, and T. Lee, "Geometric nonlinear PID control of a quadrotor UAV on $SE(3)$," *arXiv preprint arXiv:1304.6765*, 2013.

[11] B. Vang and R. Tron, "Geometric attitude control via contraction on manifolds with automatic gain selection," in *2019 IEEE 58th Conference on Decision and Control (CDC)*. IEEE, 2019, pp. 6138–6145.

[12] M. Greiff, Z. Sun, and A. Robertsson, "Tuning and analysis of geometric tracking controllers on $SO(3)$," in *2021 American Control Conference (ACC)*. IEEE, 2021, pp. 1674–1680.

[13] F. Aslam and M. F. Haydar, "Robust attitude tracking on the Special Orthogonal Group $SO(3)$ using PD-type state feedback and linear matrix inequalities," *European Journal of Control*, p. 100689, 2022.